One-dimensional Direct Vlasov Simulations of Non-stationary Plasma Expansion in Magnetic Nozzle

IEPC-2017-106

Presented at the 35th International Electric Propulsion Conference
Georgia Institute of Technology – Atlanta, Georgia – USA
October 8–12, 2017

G. Sanchez-Arriaga*, J. Zhou† and E. Ahedo‡
Universidad Carlos III de Madrid, Leganés, Madrid, 28911, Spain

M. Martínez-Sánchez§ and J.J. Ramos ¶
Massachusetts Institute of Technology, Cambridge, 02139, Massachusetts, USA

The one-dimensional (paraxial approximation) transient expansion into vacuum of a collisionless electron-ion plasma guided by a magnetic nozzle is studied numerically. The simulation box, initially empty, has zero boundary conditions for the gyrocenter distribution functions of electrons and ions $\bar{f}_e$ and $\bar{f}_i$, except at the entry of the nozzle, where particles with a positive axial velocity follow a Maxwellian. The time evolutions of $\bar{f}_e$ and $\bar{f}_i$ are computed with a parallelized direct Vlasov code, which solves a non-stationary guiding center equation for fully magnetized plasmas and discretizes the distribution functions in phase space. The latter involves the (conserved) magnetic moment, and the axial coordinate and velocity of the particles. The gyrocenter distribution functions of the electrons and the ions, affected by the axial components of the electrostatic electric field and the gradient of the magnetic field strength, are coupled through Poisson equation in the code. The evolution of macroscopic quantities, like particle density and electrostatic potential profiles, are discussed. Relevant kinetic features, such as the evolution of the ions towards a mono-energetic distribution function and the evolution of the plasma temperature profiles, are analyzed. The electron trapping, which the stationary models cannot determined self-consistently, and the transient trapping mechanism are captured by the code. This allows an assessment of the impact of the population of trapped electrons and a detailed analysis of their distribution function in terms of axial position, velocity and magnetic moment. Extensions of the code to two-dimensional configurations with axisymmetric geometry, but still fully magnetized plasmas, are discussed.

*Ramón y Cajal Research Fellow, Bioengineering and Aerospace Engineer Department, gonzalo.sanchez@uc3m.es
†PhD candidate, Bioengineering and Aerospace Engineer Department, jzhou@pa.uc3m.es
‡Full Professor, Bioengineering and Aerospace Engineer Department, eduardo.ahedo@uc3m.es
§Professor Emeritus, Department of Aeronautics and Astronautics, mmart@mit.edu
¶Principal Research Scientist, Plasma Science and Fusion Center, ramos@psfc.mit.edu

Nomenclature

B	= magnetic field
$\boldsymbol{E}$	= electric field
f	= gyrocenter distribution function
H	= particle energy
I	= total plasma current
j	= current density
P	= local plasma pressure
R_L	= current loop radius
B_0	= magnetic field at the nozzle throat
T	= local plasma temperature
z	= axial coordinate
n	= local plasma density
N_0	= plasma density at the reservoir
Q	= local heat flux
t	= time
u	= average parallel velocity
$v_\parallel$	= axial velocity
z_0	= axial coordinate of the nozzle entrance
z_M	= maximum axial distance of the computational domain
Z	= charge number
β	= particle-to-electron mass ratio
δ	= particle-to-electron temperature ratio
ϕ	= electrostatic potential
λ_{De}	= electron Debye length
μ	= magnetic moment
ω_{pe}	= electron plasma frequency

Subscripts

$\alpha = e, i$	= electrons, ions
M	= variables at z_M
T	= variables at the throat of the nozzle
$\parallel$	= along the magnetic field lines
$\perp$	= normal to the magnetic field lines

I. Introduction

Several types of thrusters in electric propulsion, such as the helicon plasma thruster,[1] the magnetoplasma-dynamic thruster,[2] and the Variable Specific Impulse Magnetoplasma Rocket (VASIMR)[3] involve magnetic nozzles. Permanent magnets or electromagnetic coils are used to create an applied magnetic field that guides the plasma expansion. The mass and simplicity penalty introduced by the nozzle is compensated by a gain on thruster efficiency. The nozzle acts as a contactless and effective wall that confines, accelerate, and guide the plasma. Thanks to this device, part of the internal energy of the electrons is transferred through a self-consistent electric field to the ions, which gain a higher axial kinetic energy. Therefore, more thermal energy can be converted into directed kinetic energy by using the nozzle. Conventional magnetic nozzles consist in an axisymmetric, convergent-divergent magnetic field. Non-symmetric configurations to deflect the plasma jet laterally and provide thrust vector control with no moving parts have been also proposed.[4]

Interesting plasma phenomena, such as the physical mechanisms transforming electron thermal energy into ions directed kinetic energy, the plasma detachment, and the role played by the plasma induced magnetic field, have been studied using fluid descriptions.[5–10] However, the validity of the heat fluxes models used to close the fluid system are doubtful. A recent work on fully magnetized and stationary plasmas provided self-consistent kinetic solutions for the first time.[11] The authors used the existence of two invariants, i.e. conservation of the energy and the magnetic moment, to write the electron and ion densities as a function of the electrostatic potential ϕ. Inserting these results in the quasi-neutrality condition provides an equation for ϕ that can be solved numerically. An important limitation of this method is that it only provides the densities of the particles connecting with the plasma reservoir. In other words, it only incorporates particles whose trajectories connect with the entrance of the nozzle if integrated backwards in time under the effect of the stationary electrostatic potential. Since convergence issues were found in the numerical algorithm of the quasineutrality condition with just these particles, the authors incorporated a population of doubly-trapped electrons. After filling with a Maxwellian distribution function all the regions of the phase space allowing trapped electrons, they were able to find numerical solutions.

Particle trapping takes place during the transient and also due to collisions. Therefore, stationary and collision-less theories are not able to incorporate them self-consistently. Several areas in plasma physics have to face the same problem and a possible solution is the implementation of costly numerical simulations. For instance, it was argued that a population of trapped electrons should exist at the ram side of an electron-attracting Langmuir probe in flowing plasma,[12] and such a population has been recently detected by running non-stationary direct (eulerian) Vlasov simulations.[13] In the case of plasma expansion under the presence of magnetic field, adiabatic trapping in slowly varying time-dependent electric fields[14] were also considered.[15] Non-stationary particle-in-cell simulations, which have been also adapted to incorporate particle collisions,[16] constitute an alternative to study the particle trapping.

This work is focussed on the particle trapping occurring during the transient phase of a plasma expansion in a magnetic nozzle. A novel code, which solves the non-stationary and one-dimensional Vlasov equations for the gyrocenter distribution functions of the particles coupled with Poisson's equation, has been developed and used to characterize the population of trapped particles. Other kinetic features, such as the densities, current, temperature, and pressure profiles, and also the distribution functions of the particles are presented.

II. Magnetic nozzle model

As shown in Fig. 1, we consider a plasma reservoir placed at $-\infty < z < z_0 < 0$ and filled with a Maxwellian plasma of density N_0 and electron and ion temperatures T_{e0} and T_{i0}. A current loop of radius R_L and located at $z = 0$ generates a stationary convergent-divergent magnetic field at the vacuum region with maximum at the nozzle throat $B(z = 0) = B_0$. Hereafter, axial coordinate z, time, velocities, magnetic fields, electrostatic potential, particle distribution functions, and densities, are normalized over λ_{De0}, ω_{pe0}^{-1}, $\lambda_{De0}\omega_{pe0}$, B_0, $k_B T_{e0}/e$, $N_0 \left(m_e/k_B T_{e0}\right)^{3/2}$, and N_0, respectively, where $\lambda_{De0} = \sqrt{\epsilon_0 k_B T_{e0}/N_0 e^2}$ is the Debye length, $\omega_{pe} = \sqrt{N_0 e^2/m_e \epsilon_0}$ the electron plasma frequency, k_B the Boltzmann constant, m_e the electron mass, e the elementary charge, and ϵ_0 the vacuum permittivity.

The model lies on a set of hypotheses that simplify the analysis markedly but still capture the electron trapping self-consistently. First of all, it assumes a slender and slowly-varying magnetic field, and investigate

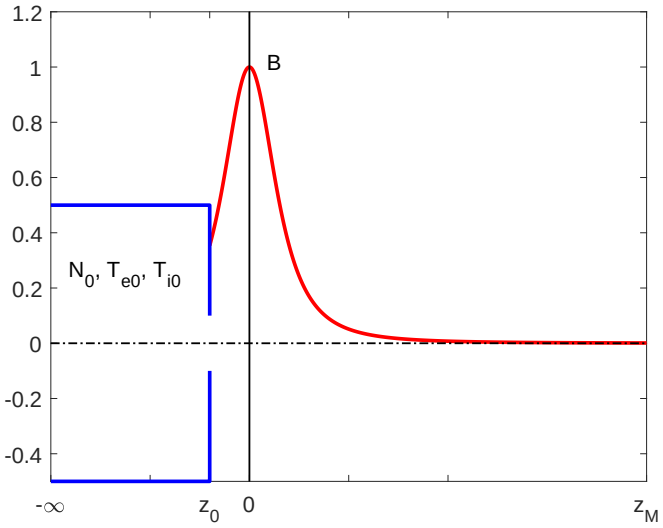

Figure 1. Geometry of the convergent-divergent magnetic nozzle.

the plasma dynamics considering the magnetic field at the axis of the nozzle, which reads

$$B = \frac{r_L^3}{\left(r_L^2 + z^2\right)^{3/2}} \mathbf{1}_z, \quad z > z_0, \tag{1}$$

with $r_L = R_L/\lambda_{De0}$ and $\mathbf{1}_z$ is an unit vector along the z-axis. Secondly, the magnetic field is so strong that the normalized Larmor radius satisfies $\rho_L \equiv \beta_\alpha v_\perp/|Z_\alpha|B << r_L$, with $v_\perp$ the normalized component of the velocity perpendicular to the magnetic field lines, and Z_α the charge number, and $\beta_\alpha \equiv m_\alpha/m_e$ the normalized mass. Our model works under the limit $\rho_L/R_L \to 0$ and ignores the slow drift motion of the particles across the field lines. The normalized magnetic moment

$$\mu = \frac{\beta_\alpha v_\perp^2}{2B} \tag{2}$$

is conserved. For brevity, we wrote $\mu_\alpha \to \mu$ in Eq. 2. Thirdly, the plasma induced magnetic field is also neglected. Under this set of hypotheses, the distribution function of the gyrocenters $\bar{f}_\alpha(t, z, v_\parallel; \mu)$ is governed by the following Vlasov equation

$$\frac{\partial \bar{f}_\alpha}{\partial t} + v_\parallel \frac{\partial \bar{f}_\alpha}{\partial z} + a_\alpha \frac{\partial \bar{f}_\alpha}{\partial v_\parallel} = 0, \tag{3}$$

with

$$a_\alpha = -\frac{1}{\beta_\alpha}\left(Z_\alpha \frac{\partial \phi\,(t,z)}{\partial z} + \mu \frac{dB\,(z)}{dz}\right) \tag{4}$$

the parallel acceleration, ϕ the normalized electrostatic potential, and $v_\parallel$ the velocity component parallel to the magnetic field line. The two Vlasov equations are coupled by the normalized electric field $\boldsymbol{E} = E_\parallel \boldsymbol{B}/B = -\partial\phi/\partial z$, which is governed by the paraxial Poisson's equation

$$B\frac{\partial}{\partial z}\left(\frac{E_\parallel}{B}\right) = \sum_{\alpha=e,i} Z_\alpha n_\alpha \tag{5}$$

with the particle densities computed from the gyrocenter distribution functions as

$$n_\alpha(z) = \frac{2\pi B}{\beta_\alpha} \int_{-\infty}^{+\infty} \int_0^{+\infty} \bar{f}_\alpha dv_\parallel d\mu. \tag{6}$$

Our numerical code integrates Eq. 3 and avoid the filamentation of the distribution function with the time splitting scheme and filter of Ref.,[17] respectively. The gyrocenter distribution functions are discretized in configuration space (eulerian or direct Vlasov solver) and the two Vlasov equations are solved in the finite domain $z_0 \leq z \leq z_M$. At z_0 we imposed the boundary conditions

$$\bar{f}_\alpha(t, z = z_0, v_\parallel > 0; \mu) = \chi_\alpha(t) \bar{f}_{M\alpha} \tag{7}$$

with

$$\bar{f}_{M\alpha} = \left(\frac{\beta_\alpha}{2\pi\delta_\alpha}\right)^{3/2} \exp\left(-\frac{\beta_\alpha v_\parallel^2}{2\delta_\alpha} - \frac{B\mu}{\delta_\alpha}\right), \tag{8}$$

$\chi_e = 1$, $\delta_\alpha \equiv T_{\alpha 0}/T_{e0}$, and $\chi_i(t)$ dynamically varied to accomplish quasineutrality at entrance section $z = z_0$ $[n_e(z_0) = n_i(z_0)]$. Therefore, the particles injected ($v_\parallel > 0$) at the entrance of the nozzle follow a Maxwellian distribution function. Downstream we set

$$\bar{f}_\alpha(t, z \to \infty, v_\parallel < 0; \mu) = 0, \tag{9}$$

i.e. we imposed no incoming ($v_\parallel < 0$) particles from the exit of the nozzle. Regarding the electrostatic potential, we set $\phi(z_0) = 0$ and $\phi(z_M) = \phi_M$, with ϕ_M a dimensionless parameter. Our initial condition for $\bar{f}_\alpha$ reads

$$\bar{f}_\alpha(t = 0, z > z_0, v_\parallel; \mu) = \bar{f}_{M\alpha} \times \exp\left(-\frac{z}{L_0}\right) \tag{10}$$

with $L_0 = 2$ a dimensionless parameter that guarantees a smooth transition at $t = 0$.

After running a simulation, we can compute the average or mean value of any quantity ψ as follows

$$\langle\psi\rangle_\alpha = \frac{1}{n_\alpha} \int \psi f_\alpha d\boldsymbol{v} = \frac{2\pi B}{\beta_\alpha n_\alpha} \int_{-\infty}^{+\infty} \int_0^{+\infty} \psi \bar{f}_\alpha dv_\parallel d\mu \tag{11}$$

The definition of the density in Eq. 6 is found by setting $\psi = 1$. Other interesting quantities are the current densities $j_\alpha = Z_\alpha N_\alpha u_\alpha$, temperatures $T_{\parallel\alpha} = \beta_\alpha \left\langle c_{\parallel\alpha}^2 \right\rangle_\alpha$ and $T_{\perp\alpha} = B \langle\mu\rangle_\alpha$, and the heat fluxes $Q_{\parallel\alpha} = \frac{1}{2}\beta n_\alpha \left\langle c_{\parallel\alpha}^3 \right\rangle_\alpha$ and $Q_{\perp\alpha} = B n_\alpha \langle\mu c_{\parallel\alpha}\rangle_\alpha$, where we introduced the peculiar velocity $c_{\parallel\alpha} = v_\parallel - u_\alpha$ and the average parallel velocity $u_\alpha = \langle v_\parallel \rangle_\alpha$.

III. Numerical Simulations

This section presents the results of a numerical simulation with physical parameters $\delta_i = 1$, $\beta_i = 100$, $Z_i = 1$, and $r_L = 50$, $z_0 = -r_L/2$, and $z_M = 800$. We remark that, although $\beta_i = 100$ is not realistic for an electron-ion plasma, it separates the electron and ion response times while helping us to save significant computational resources. For the generation of the velocity-magnetic moment grid of the electrons, we discretized the domains $-5 \leq v_{\parallel,e} \leq 5$ and $0 \leq \mu \leq 12.5$ with $N_{v_\parallel} = 77$ and $N_\mu = 101$ uniformly distributed points. For ions we used exactly the same values except that the ion velocity grid is $-0.5 \leq v_{\parallel,i} \leq 0.5$. A total of $N_z = 1051$ non-uniformly distributed points were used in the discretization of the spatial domain $z_0 \leq z \leq z_M$. Their positions were selected to keep constant the ratio between the resolution and the local Debye length, which is expected to vary as $\sim n^{-1/2} \sim B^{-1/2}$. The propagation of the distribution functions were carried out with a fixed time step equal to $\Delta t = 0.03$. Parametric analysis varying ϕ_M (not shown in this paper) revealed that the current-free condition $I = (j_e + j_i)/B = 0$ is reached in the steady state for $\phi_M = -2.75$ and that it is independent of r_L and z_M if the ratio r_L/z_M is small. Hereafter we will focus the analysis on such a particular case of special importance for electric propulsion applications.

Figure 2 shows the axial profiles of the electrostic potential and the space charge. As shown in panel (a) the electric field reaches higher values during the transient and it then relaxes to a configuration with an acceleration region close to the entrance of the nozzle, followed by a plateau and a downstream sheath. Due to the lower mass of the electrons, the space charge is negative through most of the simulation domain during the transient. As time elapses, the ions are accelerated downstream and the length of a quasineutral region increases. Moreover, a downstream sheath with positive space charge is formed in the steady state due to the truncation of the infinite domain.

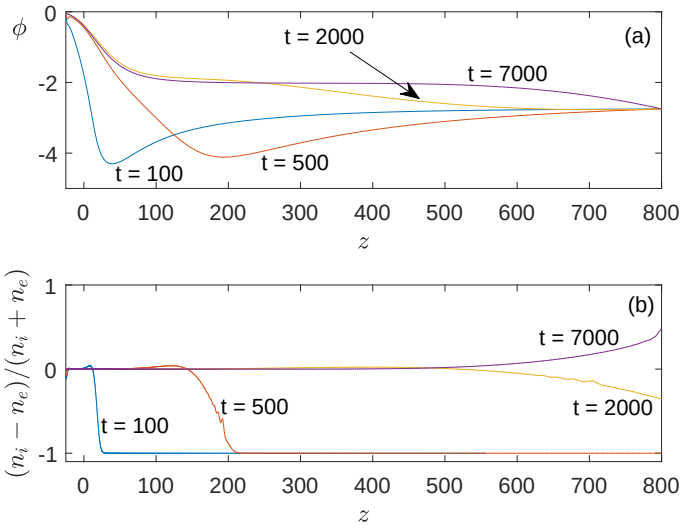

Figure 2. Panels (a) and (b) show the electrostic potential and space charge profiles at different times.

The analysis of the functions $\bar{f}_\alpha(t, z, v_\parallel, \mu)$ is not straightforward due to their four-dimensional character. In this work we extracted interesting kinetic information by plotting these functions versus z and $v_\parallel$ for a certain μ value and different times. As shown on the left panels of Fig. 3, the electron plume expands in the magnetic nozzle with a positive macroscopic velocity $u_e =< v_\parallel >_e$. Within the quasineutral region, the parallel temperature of the electrons $T_{\parallel e} = \left\langle \left(v_\parallel - u_e\right)^2 \right\rangle_e$ remains almost constant and the perpendicular $T_{\perp e} = B \left\langle \mu \right\rangle_e$ decays with B [see panels(c) and (a) in Fig. 4]. Therefore, the plasma expansion along the divergent nozzle implies both anisotropy and cooling.

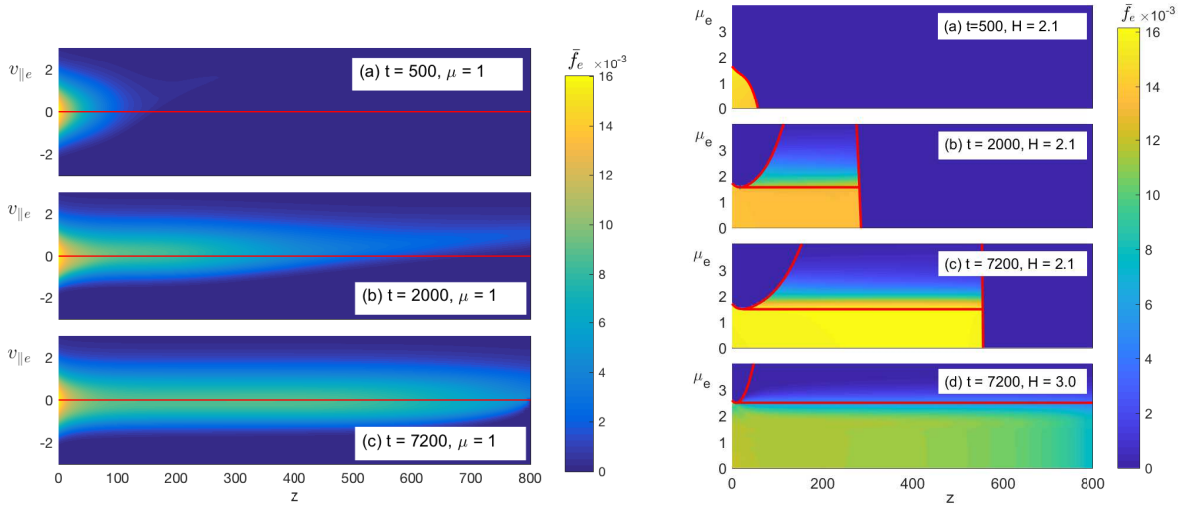

Figure 3. Left figure: electron distribution function for $\mu = 1$ at $t = 500, 2000$ and 7200 [panels (a)-(c)]. Right figure: electron distribution function at different instants and $H = 2.1$ [panels (a)-(c)] and $H = 3$ [panel (c)].

Unlike stationary models, Vlasman computes self-consistently the trapping of the electrons during the transient. For trapping analysis, it is convenient to change the variable $v_\parallel$ by the energy $H_\alpha = \beta_\alpha v_{\parallel\alpha}^2/2 + Z_\alpha \phi + \mu B$ and work with the distribution function $\bar{f}_\alpha(t, z, H_\alpha, \mu)$. The reason underlying such a change is

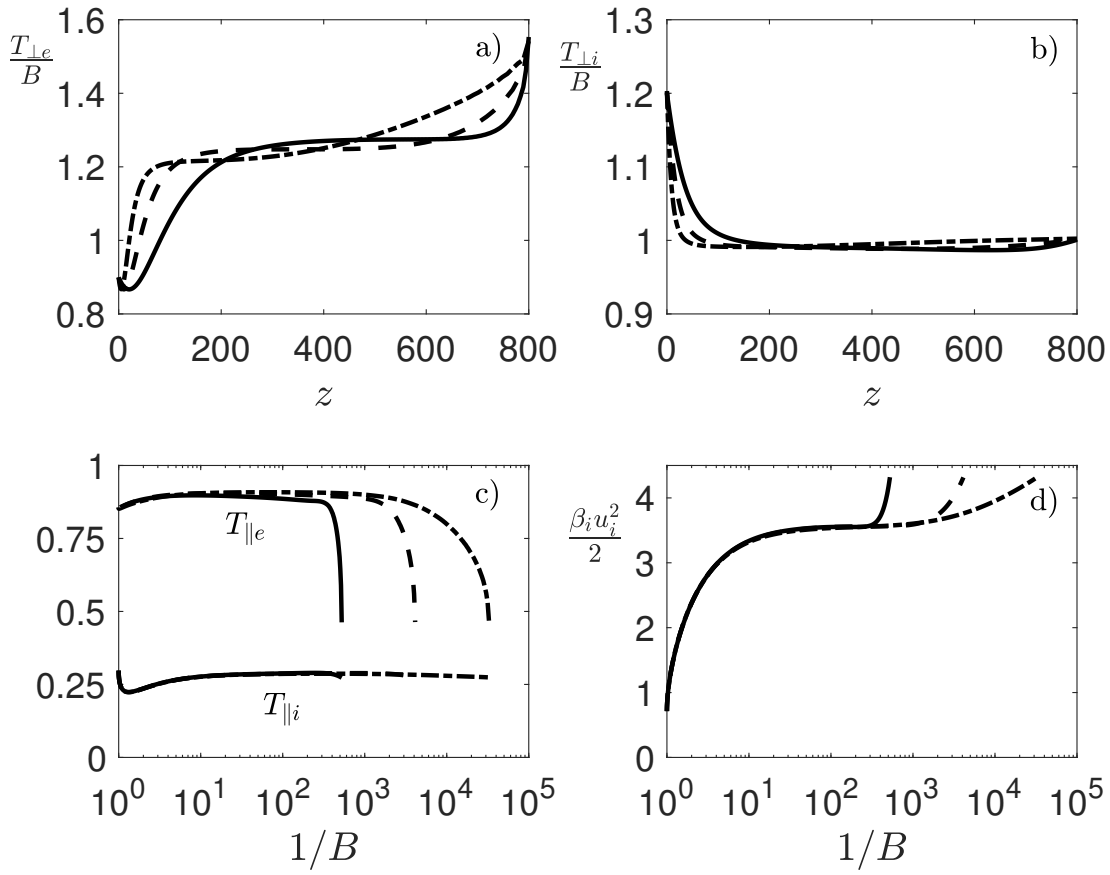

Figure 4. Panels (a) and (b) show the perpendicular temperature of the electrons and ions, respectively. Panel (c) shows their parallel temperatures and (d) the mean kinetic energy of the ions. $z_M = 800$ and solid, dashed, and dot-dash lines correspond to $r_L = 100, 50$, and 25, respectively.

the evolution law for H_α

$$\frac{dH_\alpha}{dt} = Z_\alpha \frac{\partial \phi}{\partial t}, \tag{12}$$

which is readily found from Vlasov characteristics $dz/dt = v_{\parallel\alpha}$ and $dv_{\parallel\alpha}/dt = a_\alpha(z, t, \mu)$. Therefore, under stationary conditions, the energy is conserved. At the steady state and for a given energy and z position, the maximum value of the magnetic moment

$$\mu_{max}\left(z, H\right) = \frac{H - Z_\alpha \phi}{B} \tag{13}$$

is found by setting $v_{\parallel\alpha} = 0$ in the definition of the energy. Such a curve sets an upper limit for the existence of particles in a $\mu_e - z$ diagram at a given energy (see right panels in Fig. 3) and it can exhibit a minimum at coordinates (z^*, μ^*). Three different populations of electrons are identified in these diagrams. For instance, at the end of the simulation [panel (c) with $t = 7200$ and $H = 2.1$] the electrons with magnetic moment below μ^* or above μ^* but $z < z^*$ are all reflected back to the entrance of the nozzle. A particle of energy H is trapped between two axial coordinates $z_{min} \leq z \leq z_{max}$ if its magnetic moment μ intersects the curve of μ_{max} at those points, i.e. $\mu_{max}\left(z_{min}, H\right) = \mu_{max}\left(z_{max}, H\right) = \mu$. Therefore, electrons with $\mu > \mu^*$ in panels (b) and (c) between those positions are doubly trapped. In the steady state and for higher energy [see panel (d) with $H = 3$], the electrons are free to propagate downstream and leave the simulation box if $\mu < \mu^*$. As shown in panel (c), the doubly-trapped electrons do not fill completely all the allowed phase space but only a region contiguous to μ^*. A previous stationary model filled that region completely.[11] Results of VLASMAN,

which are not presented in this paper, show that the population of trapped electrons is about 20% of the total and it depends on the particular transient followed by the system.

On the other hand, ions (see left panel in Fig. 5 and panel (d) in Fig. 4) reach a macroscopic velocity of $u_i =< v_\parallel >_i \approx 0.25$. Similarly to electrons, the ion parallel temperature $T_{\parallel i} = \beta_i \left\langle \left(v_\parallel - u_i\right)^2 \right\rangle_i$ in the quasineutral region is almost constant and equal to 0.25 and the perpendicular $T_{\parallel i} = B \langle \mu \rangle_i$ also decays with B [see panels (c) and (a) in Fig. 4]. Ions are close to monoenergetic. As shown in the right panels of Fig. 5, all the ions are free, i.e. they are accelerated downstream and leaves the simulation box. Note that $\beta_i a_i = -\left(Z_i \partial\phi/\partial z + \mu dB/dz\right) > 0$ for any μ, z.

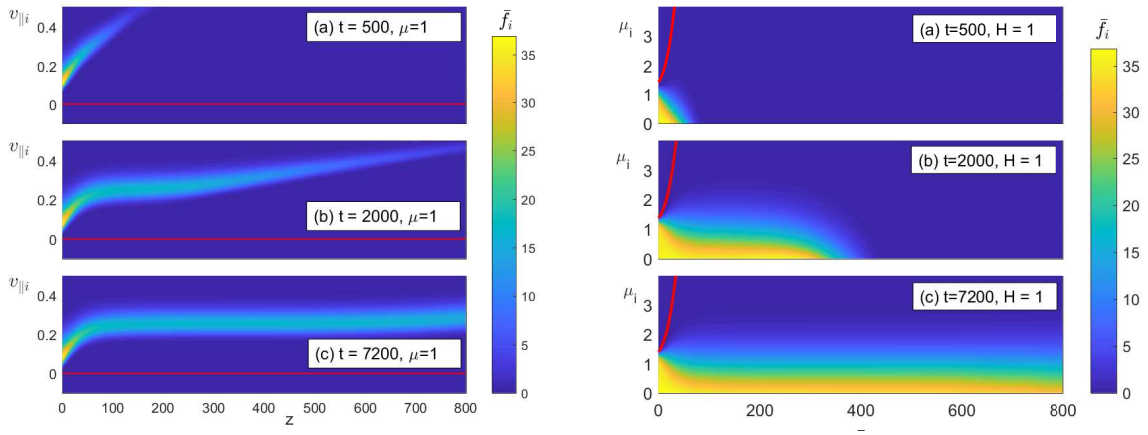

Figure 5. Left figure: ion distribution function for $\mu = 1$ at $t = 500, 2000$ and 7200 [panels (a)-(c)]. Right figure: ion distribution function at different instants and $E = 1$.

IV. Conclusion

A novel eulerian code for solving the Vlasov-Poisson system has been used to study the non-stationary and collisionless plasma expansion in a magnetic nozzle. One of the main novelties of the algorithm is the self-consistent computation of the population of doubly trapped electrons during the transient phase. The simulations, which have been carried out by setting the total potential drop that yields zero net current, show the formation of a quasineutral region and a sheath downstream. The analysis of the plasma temperatures indicates that the expansion along the divergent nozzle implies both anisotropy and cooling and the distribution function of the ions is close to mono-energetic. While all ions are accelerated downwards in the divergent nozzle, the dynamics of the electron is more complex and three different populations exist. The analysis of the electron distribution function at the steady state, which is performed in the axial coordinate versus magnetic moment plane for constant energy, shows that electrons can (i) be reflected back to the nozzle entrance, (ii) be doubly trapped and bouncing between two axial coordinates, or (iii) in the case of the most energetic, move downwards and leave the simulation box. Electrons are trapped during the transient, when the time dependent electrostatic potential varies and modifies the phase space region corresponding to trapped electrons. The simulations showed that the density of trapped electrons can represent a 20% of the total. However, the exact amount of trapped particles and its effect on the final plasma configuration depends on the history of the system and how it reaches the steady state. Therefore, such a value is not universal and the steady state of the magnetized collisionless plasma is not unique. The role played by collisions, a topic that will be investigated in future works, can change this conclusion.

Acknowledgments

G.S-A was supported by the Ministerio de Economía y Competitividad of Spain (Grant RYC-2014-15357). J.Z. was supported by Airbus DS (Grant CW240050). J.R. and M.M-S stays at UC3M for this research were supported by a UC3M-Santander Chair of Excellence and by National R&D Plan (Grant ESP2016-75887), respectively. E.A. was supported by the MINOTOR project, that received funding from the European Unions

Horizon 2020 research and innovation programme, under grant agreement 730028.

References

[1]Christine Charles and Rod Boswell. Current-free double-layer formation in a high-density helicon discharge. *Applied Physics Letters*, 82(9):1356–1358, 2003.

[2]Mariano Andrenucci. *Magnetoplasmadynamic Thrusters*. John Wiley & Sons, Ltd, 2010.

[3]Alexey V. Arefiev and Boris N. Breizman. Theoretical components of the vasimr plasma propulsion concept. *Physics of Plasmas*, 11(5):2942–2949, 2004.

[4]Mario Merino and Eduardo Ahedo. Contactless steering of a plasma jet with a 3d magnetic nozzle. *Plasma Sources Science and Technology*, 26(9):095001, 2017.

[5]Donal L. Chubb. Fully ionized quasi-one-dimensional magnetic nozzle flow. *AIAA Journal*, 10(2):113–114, 1972.

[6]Alexey V. Arefiev and Boris N. Breizman. Magnetohydrodynamic scenario of plasma detachment in a magnetic nozzle. *Physics of Plasmas*, 12(4):043504, 2005.

[7]E. Ahedo and M. Merino. Two-dimensional supersonic plasma acceleration in a magnetic nozzle. *Physics of Plasmas*, 17(7):073501, 2010.

[8]Mario Merino and Eduardo Ahedo. Plasma detachment in a propulsive magnetic nozzle via ion demagnetization. *Plasma Sources Science and Technology*, 23(3):032001, 2014.

[9]Mario Merino and Eduardo Ahedo. Effect of the plasma-induced magnetic field on a magnetic nozzle. *Plasma Sources Science and Technology*, 25(4):045012, 2016.

[10]Heath Lorzel and Pavlos G. Mikellides. Three-dimensional modeling of magnetic nozzle processes. *AIAA Journal*, 48(7):1494–1503, 2010.

[11]M. Martinez-Sanchez, J. Navarro-Cavallé, and E. Ahedo. Electron cooling and finite potential drop in a magnetized plasma expansion. *Physics of Plasmas*, 22(5):053501, 2015.

[12]Juan Ramón Sanmartín Losada. Active charging control and tethers. In C.P. Catani, editor, *Space environment : prevention of risk related to spacecraft charging : Space technology course*, pages 515–533. Cépadues, Tolouse, 2002.

[13]G. Sánchez-Arriaga and D. Pastor-Moreno. Direct vlasov simulations of electron-attracting cylindrical langmuir probes in flowing plasmas. *Physics of Plasmas*, 21(7):073504, 2014.

[14]A. V. Gurevich. Distribution of Captured Particles in a Potential Well in the Absence of Collisions. *Soviet Journal of Experimental and Theoretical Physics*, 26:575, March 1968.

[15]M. A. Raadu. Expansion of a plasma injected from an electrodeless gun along a magnetic field. *Plasma Physics*, 21(4):331, 1979.

[16]Albert Meige, Rod W. Boswell, Christine Charles, and Miles M. Turner. One-dimensional particle-in-cell simulation of a current-free double layer in an expanding plasma. *Physics of Plasmas*, 12(5):052317, 2005.

[17]C. Z. Cheng and Georg Knorr. The integration of the vlasov equation in configuration space. *Journal of Computational Physics*, 22(3):330 – 351, 1976.